Applied Physics Letters

Manipulation of ferroelectric domain inversion and growth by optically induced 3D thermoelectric field in lithium niobate

Cite as: Appl. Phys. Lett. **121**, 181111 (2022); https://doi.org/10.1063/5.0106711
Submitted: 29 June 2022 • Accepted: 20 October 2022 • Published Online: 04 November 2022

Xiaoliang Wang, Qiang Cao, Ruonan Wang, et al.

AIP Publishing

Applied Physics Letters ARTICLE scitation.org/journal/apl

Manipulation of ferroelectric domain inversion and growth by optically induced 3D thermoelectric field in lithium niobate

Cite as: Appl. Phys. Lett. **121**, 181111 (2022); doi: 10.1063/5.0106711
Submitted: 29 June 2022 · Accepted: 20 October 2022 ·
Published Online: 4 November 2022

Xiaoliang Wang,[1] Qiang Cao,[1,a)] Ruonan Wang,[1] Xiangdong Cao,[2] and Sheng Liu[1]

AFFILIATIONS

[1]The Institute of Technological Sciences, Wuhan University, Wuhan 430072, China
[2]Center for Optics Research and Engineering of Shandong University, Shandong University, Jinan 250100, China

[a)]Author to whom correspondence should be addressed: caoqiang@whu.edu.cn

ABSTRACT

We experimentally demonstrate the use of a femtosecond laser-induced thermoelectric field to manipulate remotely—not only at the focal spot—the inversion and growth of ferroelectric domain in lithium niobate. The process involves two steps: the first step is laser marking, in which a laser is used to mark the origin of the desired domain inversion. The second step is laser induction, in which a laser-induced thermoelectric field is used to invert the domain at the marker site and drive domain growth. The induced thermoelectric field is distributed in three dimensions, which can simultaneously manipulate the domain inversion and growth length of multiple marked sites within a diameter of ~200 μm. The length of domain growth is synergistically controlled by the position and intensity of marking and induction, which can exceed 100 μm. This two-step poling method greatly improves the efficiency of all-optical poling and provides a different suite of tools for tailoring ferroelectric domains.

Ferroelectrics are materials with spontaneous polarization, which can be inverted below the Curie temperature. The polarization inversion reverses the sign of the second-order nonlinear tensor and the Pockels electro-optical tensor of the material.[1] Ferroelectric materials have been exploited in various areas of nonlinear optics, optoelectronics, nonvolatile memory, quantum communication, and biomedicine by manipulating ferroelectric polarization and associated domains.[2–6] Electric field poling is the most common method for ferroelectric domain inversion via applying an electric field in excess of the coercive field along the polar axis of crystals. The widely used periodically poled lithium niobate (PPLN) is achieved using this method. However, the electric field poling is cumbersome as it requires tailored masks to determine the shape and period of the domain engineering.[7] Moreover, it is laborious to deal with thick crystals and fabricating fine domains with high aspect ratios,[8] and impossible to create isolated domains in ferroelectrics.

Optical poling is an attractive field because of its facile process, remote manipulation, high spatial resolution, and 3D fabrication capability.[9] All-optical poling involves mainly UV light and focused infrared femtosecond laser. UV light can invert ferroelectric domains on the crystal surface through a strong absorption-induced thermoelectric or pyroelectric field, but only to a depth of a few hundred nanometers.[10] However, infrared femtosecond laser can focus inside the transparent material to induce domain inversion. For example, by direct laser writing in lithium niobate ($LiNbO_3$) to fabricate arbitrary two-dimensional domain structures, but in the report, the domain length only reaches ~60 μm.[11] Additionally, the fabrication is time-consuming as it takes 10 s to induce a 100 μm domain at a speed of 10 μm/s, which is clearly not suitable for large-scale domain engineering.

Femtosecond laser poling also enables the fabrication of three-dimensional (3D) domain inversion structures in some ferroelectrics, such as in barium calcium titanate, $Ba_{0.77}Ca_{0.23}TiO_3$, calcium barium niobate, and tetragonal PMN-38PT.[12–15] These results advance quasi-phase matching to three dimensions, thus realizing applications such as 3D nonlinear photonic crystals and nonlinear wavefront shaping. The mechanism of femtosecond laser poling is that the nonlinear absorption of light generates a high-temperature gradient in materials. The temperature gradient induces a thermoelectric field due to the thermoelectric effect. When the thermoelectric field is larger than the coercive field, it reverses the ferroelectric domain.[16] However, only the electric field at the laser focus is usually used for poling, while the electric field in other regions is not used. Therefore, using this method,

the domain can only be created at the focal spot. Fabricating long domain structures with period reversal is necessary to move the focal point repeatedly.

In addition to reversing ferroelectric domains, a femtosecond laser can create modified regions with a lower nonlinear coefficient in the crystal.[17,18] The nonlinear coefficient of the modified region decreases due to the disruption of the crystal structure.[19] The laser modification method also allows the fabrication of 3D domain structures, but the nonlinear conversion efficiency in quasi-phase matching is lower than that of periodically poled structures.[20,21] Laser fabrication of modified domains in ferroelectrics seems beneficial for inducing domain inversion. For example, fabricating modified domains in $LiNbO_3$ followed by overall heat treatment can induce domain inversion above or below the modified domains.[22] The domain inversion is up to 800 μm in length, much larger than that induced by femtosecond laser only. However, the modified region is 200 μm long, severely damaging the crystal. The main contribution to the reversal of the ferroelectric domain is the additional heat treatment rather than the laser. Considering that the high temperature induced in the crystal during femtosecond laser poling is spatially distributed in three dimensions,[23] a similar localized heat treatment can be formed. Therefore, it is possible to explore the use of the laser-induced 3D thermoelectric field to tailor multi-domain inversion with the assistance of modified domains, which is important for large-scale domain engineering.

Here, we experimentally demonstrate an all-optical poling method in $LiNbO_3$ crystal, named as two-step laser poling. The first step, laser marking (LM), uses laser modification to mark the origin of the desired domain structures. The second step, laser induction (LI), uses multiple laser pulses to induce a 3D thermoelectric field inside the crystal. We show the ability of the laser-induced 3D thermoelectric field to manipulate domain inversion and growth at a marked site remotely. The manipulation characteristics of LI energy for different marked sites are investigated, and thus, three manipulation ways are introduced. The 3D thermoelectric field is exhibited to manipulate ferroelectric domains within a diameter of ~200 μm. After designing the marked sites, we achieve tailored multi-domain structures under a single LI. This method is also suitable for other popular ferroelectrics.

In the experiment, the samples are z-cut 5% MgO-doped $LiNbO_3$ crystal with a thickness of 500 μm. The sample is mounted onto a high-precision displacement holder (Aerotech Inc.) equipped with a PC-driven three-axis XYZ crossed-roller bearing positioning system. A universal femtosecond laser fabrication system is used for marking and induction. Light is derived from a regenerative amplified Yb:KGd(WO4)2 (KGW)-based laser system (Pharos, Light Conversion) outputting light with a wavelength of 1026 nm, a pulse duration of 170 fs, and a repetition rate of 1000 kHz. The pulse energy can be continuously adjustable from 0 to 400 μJ through an attenuator consisting of a half-wave plate and a polarizing plate. Focusing the laser with a 50× microscope objective (NA = 0.42) produces a focal spot diameter of approximately 1–2 μm. The light polarization is along the X-axis of the crystal during processing. The fabricated domain structures, including modified and inverted domains, are observed by Čerenkov-type SH confocal microscopy (FVMPE-RS, Olympus), which allows for nondestructive characterization.[24,25]

The principle of the two-step laser poling method is shown in Fig. 1. We first use the LM to create a tiny modified domain on the +z-surface of the $LiNbO_3$ crystal. Then, multiple laser pulses are

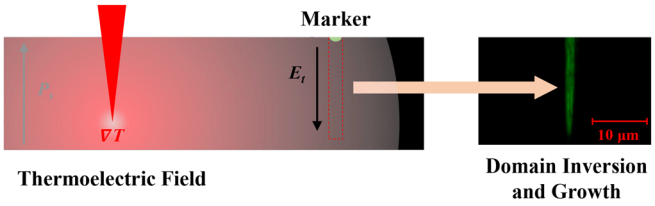

FIG. 1. Laser-induced thermoelectric field remotely manipulates domain inversion and growth (Čerenkov SH microscopy image) at the marked site. P_s indicates spontaneous polarization.

focused away from the modified domain to generate high-temperature gradients ∇T. The temperature gradient induces a 3D thermoelectric field. If the electric field E_t near the marked site is larger than the coercive field here, it reverses the ferroelectric domain and drives the domain growth. In the previous laser poling approaches, such a long domain must be fabricated by focal scanning. The modified domain processed by the LM plays a locational role, and we guess there are two reasons for this. One is the presence of the modified domain reduces the coercive field due to the domain walls trapping electric charges.[22,26] Second is the region around the modified domain may serve as nucleation sites.[27–29] Modified domains are permanent defect structures and therefore very stable.

Based on this principle, we can use the laser-induced 3D thermoelectric field to simultaneously manipulate domain inversion and growth at multiple marked sites, as shown in Fig. 2(a). We used an LM with a pulse number of 1 and a pulse energy of 150 nJ to fabricate three marked rings with diameters of 20, 30, and 40 μm on the crystal surface. Then, a thermoelectric field is induced in the center of the rings 20 μm below the crystal surface using LI with a pulse number of 500 000 and pulse energies of 300, 400, 500, 600, 700, 800, and 900 nJ, respectively. The experimental results are shown in Fig. 2(b). The proportion of domain inversion occurrence and the length of domain growth at the marked sites on different rings are shown in Figs. 2(c) and 2(d), respectively.

The marked areas show slight ablation since the LM energy exceeds the crystal damage threshold, as shown in the upper right corner of Fig. 2(b). When the LI energy is below 400 nJ, the induced electric field is so weak that it only sporadically reverses the ferroelectric domain at the marked sites of the inner ring. When the energy reaches 400 nJ, the proportion of domain inversion on the inner ring increases to ~30%. As the energy increases, many of marked sites on the inner ring occur where domain inversion. When the energy is 900 nJ, the proportion of domain inversion is 100%. As the LI energy increases, a similar trend is observed for the marked sites on the middle and outer rings. The difference is that the minimum LI energy required to manipulate multi-domain inversion is raised to 600 and 700 nJ, respectively, and the proportion of domain inversion is not as high as that on the inner ring. These reflect two points. One is the randomness of the "quality" of the markers, and each site has a different coercive field. Second, the strength and scope of the electric field increase with the LI energy.

In terms of the variation of the average length of domain growth with the LI energy, the domains on the inner and middle circles become shorter, decreasing approximately from 80 to 10 μm and from 30to 15 μm, respectively. While the domain length on the outer circle

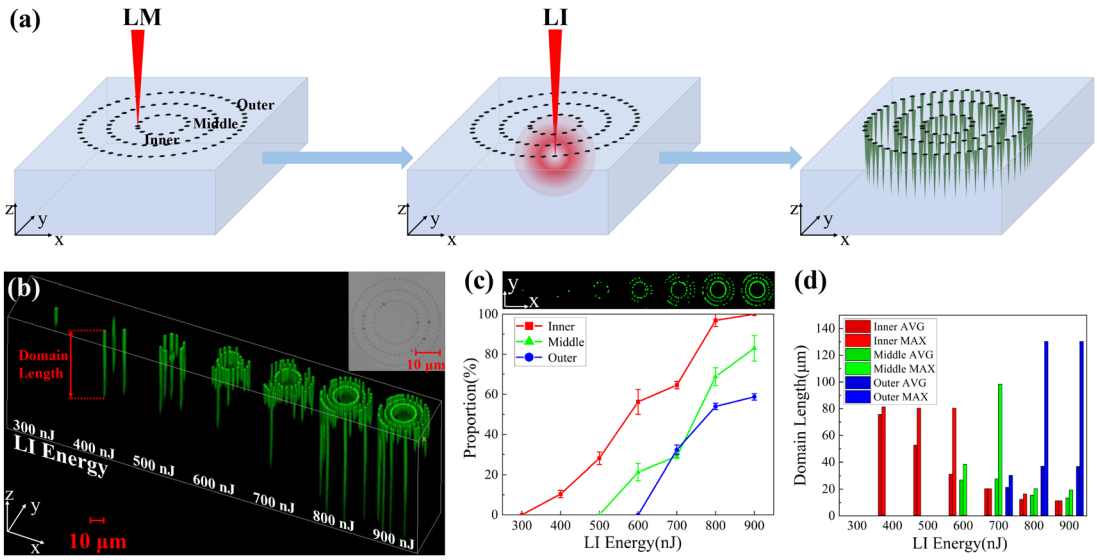

FIG. 2. (a) Laser-induced thermoelectric field simultaneously manipulate multiple marked sites for domain inversion and growth. (b) Manipulation results of LI with different pulse energies visualized by Čerenkov-type SH confocal microscopy. (c) The proportion of domain inversion occurrence and (d) the average length of domain growth on the inner, middle, and outer marked rings at different LI energies. AVG indicates the average value. MAX indicates the maximum value.

becomes longer, increasing from 20 to 40 μm. When the LI energy is 700 nJ, the length of the domains on the three circles is approximately equal. The longest domains are more likely to appear in the outermost layer of the group domain for all LI energies considered, with a typical length of 80 μm and up to 130 μm. The variation is due to the fact that the laser-induced electric field is a bipolar field oriented from the low-temperature to the high-temperature region,[14] which means that the electric field in the opposite direction below the poling electric field inhibits domain growth. The domain growth is driven by not only the thermoelectric field but also the energy of the displaced atoms after the domain inversion. When the energy (including kinetic and potential energy) is greater than the opposite-direction electric field, the domain will continue to grow and, thus, exceed the depth of LI.

The LI can manipulate not only the marker sites on the surface but also the inside of the crystal. There are two kinds of results, as shown in Fig. 3(a). One is unidirectional growth: the inverted domain grows from the marked site to the surface. The other is bidirectional growth: the inverted domain grows not only from the marked site to the surface but also to the inside. We fabricated three marked rings of the same size at 5 μm below the +z-surface using an LM with a pulse number of 1 and pulse energy of 500 nJ. Then manipulated with the same LI arrangement, the experimental results are shown in Figs. 3(b)–3(d).

As the LI energy grows, the proportion of domain inversion on the three rings tends to increase and decrease. Still, their ordering—unlike in Fig. 2(c)—shows a complex variation, which implies the changes in the laser-induced electric field. The proportion of domain inversion on the inner, middle, and outer rings reaches their highest values at LI energies of 600, 700, 700 nJ, respectively, corresponding to ∼60%, ∼40%, and ∼80%, respectively. Although the focal center of LI boasts a high temperature, the temperature gradient is close to zero. Therefore, the electric field generated by the high-energy LI at each marked site gets weaker, resulting in a lower domain inversion proportion.

Notably, when the LI energy is less than a certain threshold, such as 600 nJ in this experiment, the induced electric field only drives the growth of domains at all marked sites toward the crystal surface, which provides a way to tailor the domain structures quickly. As shown in Fig. 4(a), complex domain structures are created by a single LI after designing the positions of all the markers. Figures 4(b) and 4(c) show two other examples we have made using this way. The appropriate adjustment range for the depth of LM is between 0 and 20 μm, and too deep LM will sharply increase the challenge of LI. During the fabrication process, the pulse energy of the LM needs to be adjusted to make the appropriate marks at different depths inside the crystal. Oversized or downsized markers will make it harder to be poled. As the LM is done with a single pulse and neither the LM nor the LI has to move the focus, the whole process is very fast and energy efficient compared to conventional all-optical poling methods. In addition, by reducing the spacing of the markers, it is capable of combining the inverted domain units, thus forming a continuous ferroelectric domain walls, as in Fig. 4(d). This implies that the two-step laser poling method has the potential to be used as an alternative to fabricating PPLN.

The laser-induced electric field has a large scope of action, as shown in Fig. 4(e), where a LI of 800 nJ can manipulate domain inversion and growth within a diameter range of ∼200 μm. Although there are still some marked sites in this result without domain inversion, it is possible to deal with this problem by optimizing the parameters and ways of LM and LI. Therefore, a single LI allows the manipulation of ferroelectric domains at thousands of sites. The domain engineering efficiency can be improved by several orders of magnitude. Furthermore, since the LI does not influence the inversion domains fabricated earlier, the method can divide a region into multiple cell modules for processing to achieve large-scale all-optical poling.

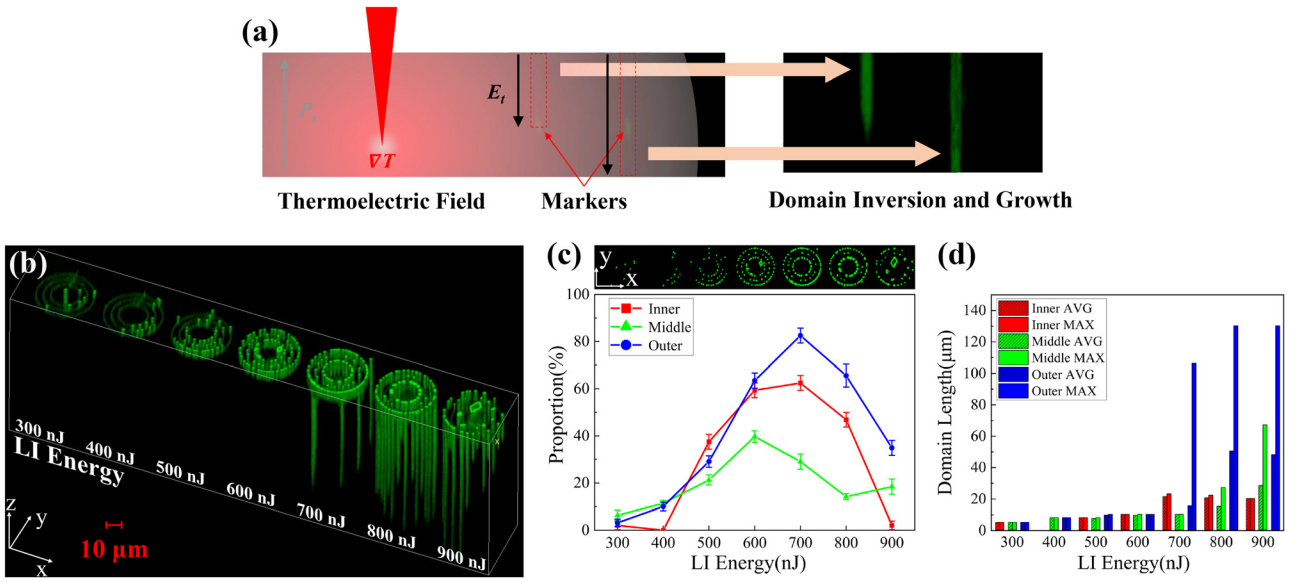

FIG. 3. (a) Two kinds of LI manipulation of domain growth when the marked site is inside the crystal. (b) Manipulation results of LI with different pulse energies visualized by Čerenkov-type SH confocal microscopy. (c) The proportion of domain inversion occurrence and (d) the average length of domain growth on the inner, middle, and outer marked rings at different LI energies.

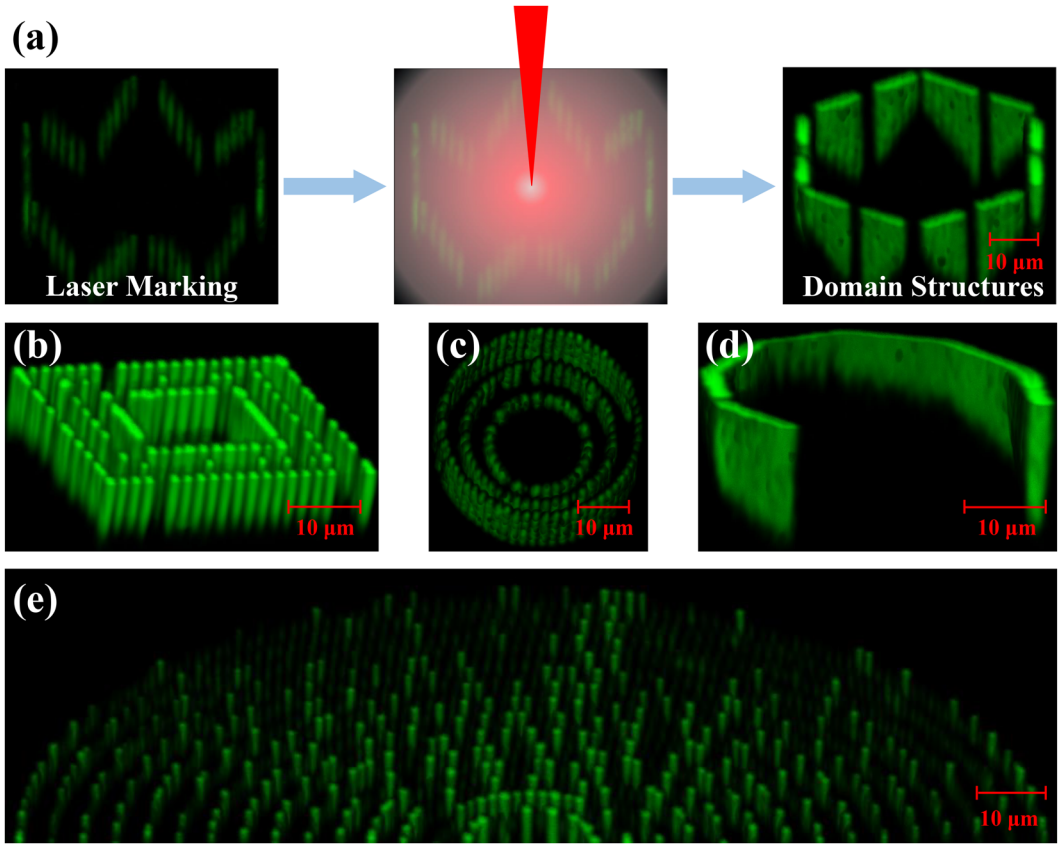

FIG. 4. (a) Rapid tailoring of complex domain structures by the two-step laser poling, and (b) and (c) other cases. (d) 3D curved domain walls. (e) Scope for manipulating domain inversion and growth by LI with a pulse energy of 800 nJ. The domain structures are visualized by Čerenkov-type SH confocal microscopy.

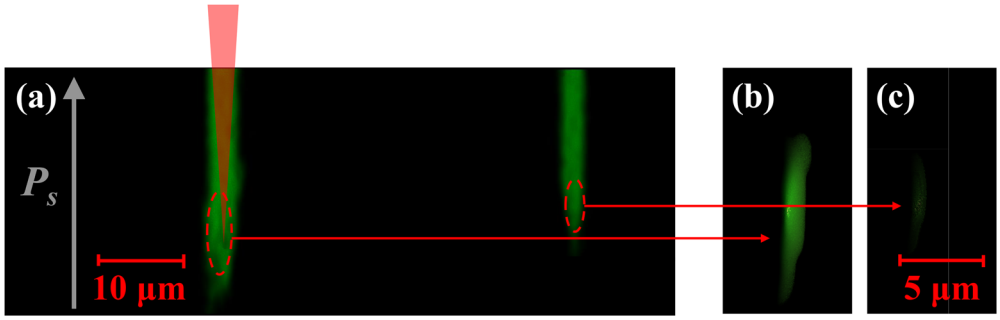

FIG. 5. (a) Use of multiple laser pulses to induce a 3D thermoelectric field while fabricating a marker, realizing simultaneous manipulation of ferroelectric domain inversion and growth (Cerenkov SH microscopy image) at the focal and non-focal sites. (b) A marker fabricated by the LI. (c) A marker fabricated by the LM.

It is worth mentioning that the difference between the LI and the LM is mainly in the number of pulses, so the LI also can fabricate markers. Therefore, the LI can fabricate a marker while inducing an electric field, which can invert the ferroelectric domains at the focal spot and drive the domain growth, as shown in Fig. 5(a). However, since the pulse number of LI is very high, its marked area is relatively large compared to the single pulse marked one, as shown in Figs. 5(b) and 5(c). The results also suggest that the femtosecond laser can drive domain growth directly from the focal spot without needing to move the focal spot.

In conclusion, we have experimentally demonstrated a femtosecond laser-induced 3D thermoelectric field to remotely manipulate the inversion and growth of ferroelectric domains at marked sites in $LiNbO_3$. An all-optical poling method for large-scale tailored domain structures was proposed. The method consists of two steps: the LM (laser marking) and the LI (laser induction). The main difference is that the LM can be done with only a single laser pulse, while the LI requires multiple laser pulses. A single LI can invert ferroelectric domains at thousands of marked sites within a region of $\sim 200\,\mu$m diameter and drive domain growth to $\sim 100\,\mu$m. Neither the LM nor the LI needs to move the focal spot during this process, so the method is very high-efficiency and energy-efficient. The markers can be set not only on the surface but also in the interior of the crystal. The domain growth can be done in three ways depending on the LI energy, offering a different suite of tools for ferroelectric domain engineering.

The work was supported by the Strategic Priority Research Program of the Chinese Academy of Sciences (Grant No. XDA25040201), the National Natural Science Foundation of China (Grant No. 51727901), and the Key Laboratory for Laser Plasmas (Ministry of Education).

AUTHOR DECLARATIONS

Conflict of Interest

The authors have no conflicts to disclose.

Author Contributions

Xiaoliang Wang: Conceptualization (equal); Data curation (equal); Investigation (equal); Writing – original draft (equal); Writing – review & editing (equal). **Qiang Cao:** Funding acquisition (lead); Project administration (lead); Supervision (lead); Writing – review & editing (equal). **Ruonan Wang:** Data curation (equal); Investigation (equal). **Xiangdong Cao:** Methodology (supporting); Writing – review & editing (equal). **Sheng Liu:** Methodology (supporting); Resources (equal); Writing – review & editing (equal).

DATA AVAILABILITY

The data that support the findings of this study are available from the corresponding author upon reasonable request.

REFERENCES

[1]D. T. Trinh, V. Shynkar, A. Arie, Y. Sheng, W. Krolikowski, and J. Zyss, Laser Photonics Rev. **9**, 214–223 (2015).
[2]V. Berger, Phys. Rev. Lett. **81**, 4136–4139 (1998).
[3]F. Xue, X. He, W. H. Liu, D. Periyanagounder, C. H. Zhang, M. G. Chen, C. H. Lin, L. Q. Luo, E. Yengel, V. Tung, T. D. Anthopoulos, L. J. Li, J. H. He, and X. X. Zhang, Adv. Funct. Mater. **30**, 2004206 (2020).
[4]R. Mankowsky, A. von Hoegen, M. Foerst, and A. Cavalleri, Phys. Rev. Lett. **118**, 197601 (2017).
[5]J. Zhao, C. X. Ma, M. Rusing, and S. Mookherjea, Phys. Rev. Lett. **124**, 163603 (2020).
[6]W. J. Wang, J. H. Li, H. Liu, and S. H. Ge, Adv. Sci. **8**, 2003074 (2021).
[7]L. E. Myers, R. C. Eckardt, M. M. Fejer, R. L. Byer, W. R. Bosenberg, and J. W. Pierce, J. Opt. Soc. Am. B **12**, 2102–2116 (1995).
[8]C. Y. J. Ying, A. C. Muir, C. E. Valdivia, H. Steigerwald, C. L. Sones, R. W. Eason, E. Soergel, and S. Mailis, Laser Photonics Rev. **6**, 526–548 (2012).
[9]J. Guo, W. Chen, H. Chen, Y. Zhao, F. Dong, W. Liu, and Y. Zhang, Adv. Opt. Mater. **9**, 2002146 (2021).
[10]A. C. Muir, C. L. Sones, S. Mailis, R. W. Eason, T. Jungk, A. Hoffmann, and E. Soergel, Opt. Express **16**, 2336–2350 (2008).
[11]X. Chen, P. Karpinski, V. Shvedov, K. Koynov, B. Wang, J. Trull, C. Cojocaru, W. Krolikowski, and Y. Sheng, Appl. Phys. Lett. **107**, 141102 (2015).
[12]L. M. Mazur, S. Liu, X. Chen, W. Krolikowski, and Y. Sheng, Laser Photonics Rev. **15**, 2100088 (2021).
[13]S. Liu, K. Switkowski, C. Xu, J. Tian, B. Wang, P. Lu, W. Krolikowski, and Y. Sheng, Nat. Commun. **10**, 3208 (2019).
[14]T. Xu, K. Switkowski, X. Chen, S. Liu, K. Koynov, H. Yu, H. Zhang, J. Wang, Y. Sheng, and W. Krolikowski, Nat. Photonics **12**, 591–595 (2018).
[15]X. Chen, D. W. Liu, S. Liu, L. M. Mazur, X. Liu, X. Y. Wei, Z. Xu, J. L. Wang, Y. Sheng, Z. Y. Wei, and W. Krolikowski, Adv. Opt. Mater. **10**(4), 8 (2022).
[16]H. Steigerwald, Y. J. Ying, R. W. Eason, K. Buse, S. Mailis, and E. Soergel, Appl. Phys. Lett. **98**, 062902 (2011).
[17]R. Osellame, M. Lobino, N. Chiodo, M. Marangoni, G. Cerullo, R. Ramponi, H. T. Bookey, R. R. Thomson, N. D. Psaila, and A. K. Kar, Appl. Phys. Lett. **90**, 241107 (2007).
[18]S. Kroesen, K. Tekce, J. Imbrock, and C. Denz, Appl. Phys. Lett. **107**, 101109 (2015).

[19]J. Thomas, V. Hilbert, R. Geiss, T. Pertsch, A. Tuennermann, and S. Nolte, Laser Photonics Rev. **7**, L17–L20 (2013).
[20]J. Imbrock, L. Wesemann, S. Kroesen, M. Ayoub, and C. Denz, Optica **7**, 28–34 (2020).
[21]D. Wei, C. Wang, H. Wang, X. Hu, D. Wei, X. Fang, Y. Zhang, D. Wu, Y. Hue, J. Lie, S. Zhu, and M. Xiao, Nat. Photonics **12**, 596–600 (2018).
[22]J. Imbrock, H. Hanafi, M. Ayoub, and C. Denz, Appl. Phys. Lett. **113**, 252901 (2018).
[23]M. Shimizu, M. Sakakura, M. Ohnishi, M. Yamaji, Y. Shimotsuma, K. Hirao, and K. Miura, Opt. Express **20**, 934–940 (2012).
[24]Y. Sheng, A. Best, H.-J. Butt, W. Krolikowski, A. Arie, and K. Koynov, Opt. Express **18**, 16539–16545 (2010).
[25]Y. Sheng, V. Roppo, K. Kalinowski, and W. Krolikowski, Opt. Lett. **37**, 3864–3866 (2012).
[26]V. Dierolf and C. Sandmann, Appl. Phys. Lett. **84**, 3987–3989 (2004).
[27]C. L. Sones, M. C. Wengler, C. E. Valdivia, S. Mailis, R. W. Eason, and K. Buse, Appl. Phys. Lett. **86**, 212901 (2005).
[28]V. Y. Shur, D. K. Kuznetsov, E. A. Mingaliev, E. M. Yakunina, A. I. Lobov, and A. V. Ievlev, Appl. Phys. Lett. **99**, 082901 (2011).
[29]M. Reich, F. Korte, C. Fallnich, H. Welling, and A. Tunnermann, Opt. Lett. **23**, 1817–1819 (1998).